

## Surface plasmons enhance optical transmission through subwavelength holes

H. F. Ghaemi, Tineke Thio, and D. E. Grupp

*NEC Research Institute, 4 Independence Way, Princeton, New Jersey 08540*

T. W. Ebbesen

*NEC Research Institute, 4 Independence Way, Princeton, New Jersey 08540  
and ISIS, Louis Pasteur University, 67000 Strasbourg, France*

H. J. Lezec

*Micrion Europe GmbH, Kirchenstrasse 2, 85622 Feldkirchen, Germany*

(Received 10 March 1998)

Optically thick metal films perforated with a periodic array of subwavelength holes show exceptional transmission properties. The zero-order transmission spectra exhibit well-defined maxima and minima of which the positions are determined by the geometry of the hole array. We show that the minima are the collection of loci for Wood's anomaly, which occurs when a diffracted beam becomes tangent to the film, and that the maxima are the result of a resonant excitation of surface plasmons (SP's). SP's from both surfaces of the metal film are apparent in the dispersion diagram, independent of which side of the film is illuminated, indicating an anomalously strong coupling between the two sides. This leads to wavelength-selective transmission with efficiencies that are about 1000 times higher than that expected for subwavelength holes.

[S0163-1829(98)06332-2]

On the surface of a metal, collective excitations of the electron density lead to the formation of surface plasmon (SP) polaritons.<sup>1</sup> Light in the visible to near-infrared range does not couple to surface plasmons on a smooth metal-air interface; however, a periodic structure allows the optical probing of the surface plasmon dispersion, in a well-defined Brillouin zone. SP polaritons have in general been observed in reflection mode on metallized gratings, appearing as an absorption feature in the intensity of a diffracted order, allowing the study of the band structure.<sup>2-8</sup>

Recently, we reported on the highly unusual *transmission* properties of metal films perforated with a periodic array of subwavelength holes.<sup>9</sup> In these samples the interaction of the incident radiation with the surface plasmons leads to an enhancement of the transmission. The zero-order transmission spectra are characterized by well-defined maxima and minima of which the positions are determined by the geometry of the hole array. Most surprisingly, we have observed transmission at wavelengths up to ten times the hole diameter with efficiencies that can exceed unity when normalized to the area of the holes, where standard aperture theory<sup>10</sup> predicts a transmission efficiency of order  $10^{-3}$ .

In this article we analyze the zero-order transmission spectra in a significant fraction of the Brillouin zone. We have identified the minima as being due to Wood's anomaly,<sup>11</sup> which is observed in diffraction gratings when a diffracted order becomes tangent to the plane of the grating. We further show that the transmission maxima are the result of a resonant excitation of surface plasmons. Moreover, we demonstrate that the surface plasmons on both sides of the metal film are excited equally strongly by the incident light. This implies that the very high transmission efficiencies observed are related to an anomalously strong coupling of the SP modes on *both* sides of the metal film through the holes.

The samples are optically thick Ag films of thickness  $0.2 \leq t \leq 0.5 \mu\text{m}$ , thermally evaporated onto a quartz sub-

strate. A Micrion 9500 focused ion beam (FIB) system was used to fabricate cylindrical cavities in a square array.<sup>9</sup> Figure 1 shows a FIB image of such an array with period  $a_0 = 900 \text{ nm}$  in an Ag film, with  $t = 200 \text{ nm}$ , and hole diameter  $d = 150 \text{ nm}$ ; the gray scale shows the grain structure of the polycrystalline film. Zero-order transmission spectra were obtained with a Cary-5 spectrophotometer using incoherent light sources with a wavelength range  $0.2 \leq \lambda \leq 3.3 \mu\text{m}$ . The sample is defined to lie in the  $(x, y)$  plane (see the inset of Fig. 3); rotating it around the  $y$  axis by  $1^\circ$  increments, up to  $\theta = 50^\circ$ , allows a study of the dispersion relation in the  $\vec{k}_x$  direction. The latter is given by  $k_x = |\vec{k}_0| \sin \theta$ , where  $|\vec{k}_0| = 2\pi/\lambda$  is the wave vector of the incident radiation;  $\lambda$  is the wavelength measured *in vacuo*. The wavelength resolution of the measurement was  $\Delta\lambda = 2 \text{ nm}$ . By placing apertures in the incident beam an angular resolution of  $\Delta\theta = 0.7^\circ$  was achieved.

We briefly mention some of the salient observations on these arrays.<sup>9</sup> The zero-order transmission spectra of an Ag

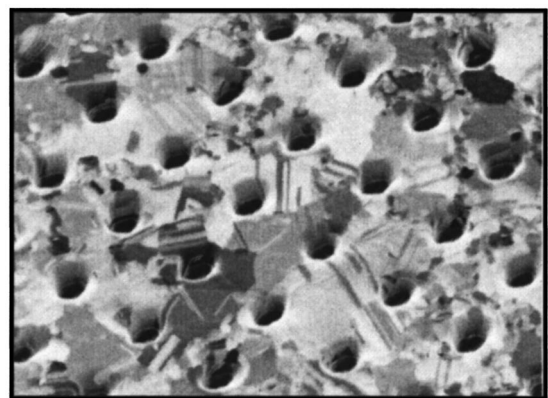


FIG. 1. Focused ion beam image of a two-dimensional hole array in a polycrystalline silver film, with film thickness  $t = 200 \text{ nm}$ , hole diameter  $d = 150 \text{ nm}$ , and period  $a_0 = 900 \text{ nm}$ .

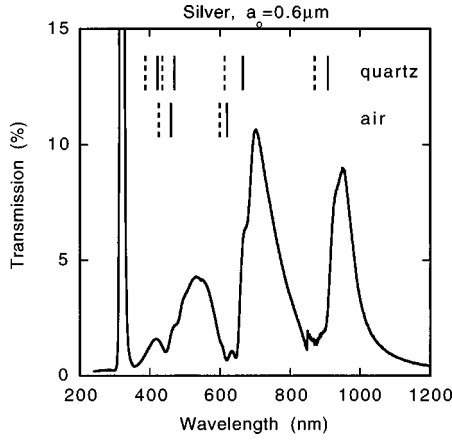


FIG. 2. Zero-order transmission of Ag film at normal incidence;  $a_0=600$  nm,  $t=200$  nm, and  $d=150$  nm. Markers indicate the wavelengths of surface plasmon modes (solid markers) and Wood's anomaly (dashed markers) at the quartz and air interfaces (upper and lower groups, respectively).

film with  $a_0=600$  nm and  $d=150$  nm is shown in Fig. 2 for normal incidence ( $\theta=0$ ). The film thickness is 200 nm, which is much larger than the skin depth ( $\sim 20$  nm) and yet too small compared to the wavelengths used to allow for waveguiding inside the cylindrical cavities. The Ag bulk plasmon is visible as a sharp resonance at  $\lambda=323$  nm, but it has no discernible influence on the rest of the spectra. At longer wavelengths, the spectrum is characterized by a set of maxima and minima of which the positions are determined by the geometry of the array, as we will discuss below. At the maxima, a surprisingly large transmission is observed, in this case  $T\sim 10\%$ . Since the holes cover  $\sim 5\%$  of the total area of the film, this corresponds to a transmission efficiency exceeding unity, when the transmission is normalized to the intensity of the light directly impinging on the holes. The results are *identical whether the illumination impinges on the quartz-metal or the air-metal interface*. The transmission properties of hole arrays fabricated in other metals, such as Al, Au or Cr, are similar. However, it is crucial that the film be metallic: In a hole array fabricated in an amorphous Ge film that is nonmetallic, the transmission efficiencies are very small at all wavelengths and limited by the absorption in the semiconductor.

A near-field scanning optical microscope (NSOM) was used to explore the intensity distribution of light emerging from the hole arrays such as the one shown in Fig. 1, when illuminated with coherent light. In the near field ( $z\approx 30$  nm) the light intensity is concentrated at the holes. The three-dimensional intensity profile obtained at distances up to  $z=300$   $\mu\text{m}$  with the NSOM is consistent with light emanating from a two-dimensional array of coherently oscillating dipoles positioned at the holes of the metal film (albeit with a surprisingly large amplitude). This is confirmed by results from a numerical simulation for  $0\leq z\leq 300$   $\mu\text{m}$  as well as from far-field diffraction experiments with coherent light sources.

The positions of both the maxima and minima in the transmission vary with the angle  $\theta$  between the normal of the sample plane and the incident wave vector  $\vec{k}_0$ . In Fig. 3 the transmitted intensity is plotted on a gray scale in the  $(E, k_x)$  plane, where the photon energy is given by  $E=hc/\lambda$ . The

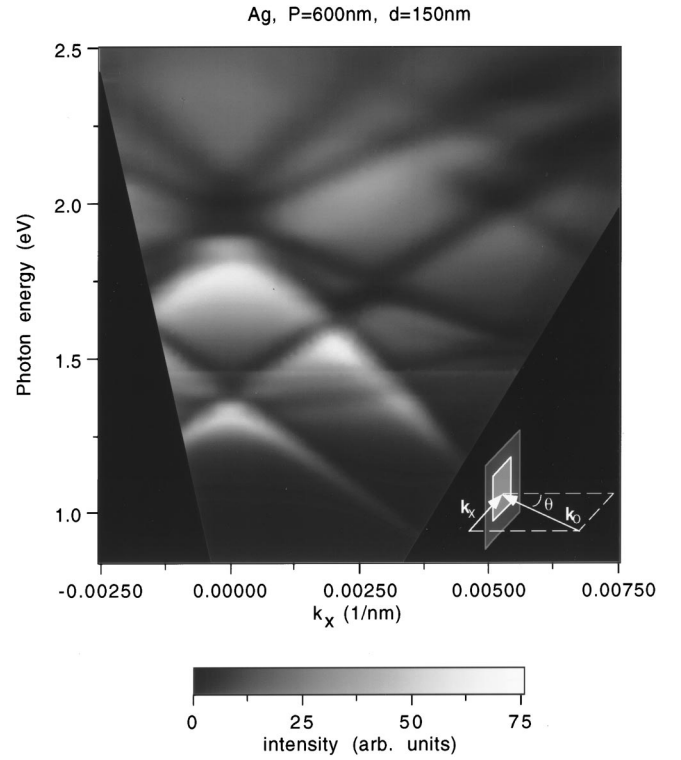


FIG. 3. Transmission intensity (gray scale; arbitrary units) as a function of photon energy and  $k_x$ . The horizontal white line at  $E\approx 1.5$  eV is an artifact of the experiment. The inset shows the geometry of the experiment.

maxima appear as a set of bright bands with fairly broad widths, whereas the minima form dark bands of which the widths are limited by the resolution of the spectrometer. The data shown in Fig. 3 are taken for  $p$  polarization (the incident electric field  $\vec{E}_0\parallel\hat{x}$ ). For  $s$  polarization ( $\vec{E}_0\parallel\hat{y}$ ), the transmission spectra are practically independent of  $\theta$ . While we pointed out earlier<sup>9</sup> that surface plasmons are involved in the exceptional transmission properties of these arrays, a more detailed analysis indicates that the spectra are actually determined by the superposition of two phenomena, namely, Wood's anomaly and the resonant excitation of the surface plasmons.

We first focus on the maxima in the zero-order transmission, which we show in the following to result from a resonant interaction of the incident light with surface plasmons on both surfaces of the metal film. The interaction is made allowed by coupling through the grating momentum<sup>1</sup> and obeys conservation of momentum

$$\vec{k}_{sp}=\vec{k}_x\pm i\vec{G}_x\pm j\vec{G}_y, \quad (1)$$

where  $\vec{k}_{sp}$  is the surface plasmon wave vector,  $\vec{k}_x$  is the component of the incident wave vector that lies in the plane of the sample as defined in Fig. 3,  $\vec{G}_x$  and  $\vec{G}_y$  are the reciprocal lattice vectors for a square lattice with  $|\vec{G}_x|=|\vec{G}_y|=2\pi/a_0$ , and  $i, j$  are integers. In order to make a comparison with the data, we use a surface plasmon dispersion appropriate for a smooth film,<sup>1</sup> ignoring in a first approximation the fact that the holes in the film may cause both a significant change in the plasmon dispersion and a large coupling between the front and back surfaces of the metal film:

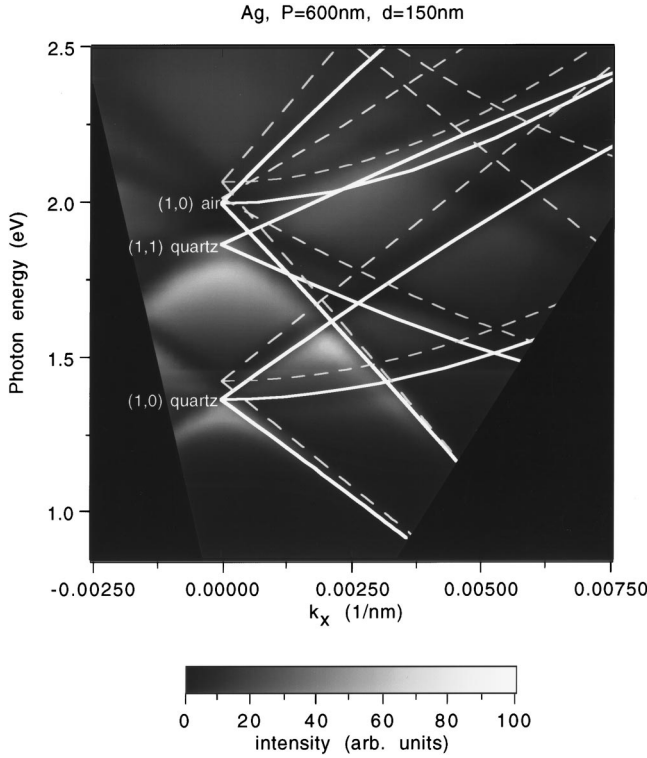


FIG. 4. Predicted energy dispersion of surface plasmons (solid lines) and loci of Wood's anomaly (dashed lines), superposed on the data of Fig. 3. The Brillouin zone boundary is at  $\pi/a_0 = 0.00524 \text{ nm}^{-1}$ .

$$|\vec{k}_{sp}| = \frac{\omega}{c} \left( \frac{\epsilon_1 \epsilon_2}{\epsilon_1 + \epsilon_2} \right)^{1/2}. \quad (2)$$

Here  $\omega$  is the frequency,  $\epsilon_1$  is the dielectric constant of the interface medium, and  $\epsilon_2$  is that of the metal. Equations (1) and (2) are solved for arbitrary  $k_x$ , taking into account the frequency dependence of the dielectric constant of silver,<sup>12</sup> to obtain the surface plasmon dispersion  $E(k_x)$  for a two-dimensionally corrugated surface with  $a_0 = 600 \text{ nm}$  shown as the solid lines in Fig. 4.

At normal incidence  $\theta = 0$ , Eqs. (1) and (2) reduce to

$$(i^2 + j^2)^{1/2} \lambda = a_0 \left( \frac{\epsilon_1 \epsilon_2}{\epsilon_1 + \epsilon_2} \right)^{1/2}. \quad (3)$$

The peak positions corresponding to selected values of  $(i, j)$  are indicated by vertical markers (solid lines) in Fig. 2. From Eq. (2) it follows that the two interfaces to the metallic film are distinguishable since  $\epsilon_1 = 1$  for air and  $\epsilon_1 = 2.16$  for the quartz substrate on which the metal film was deposited. In other words, resonant modes have different energies on the two sides, which is apparent in the spectra: When index matching fluid ( $n \approx 1.5$ ) is applied to the metal-air interface, the set of maxima associated with the metal-air interface was no longer present in the transmission spectra. As an example, the set of peaks centered at  $\lambda \approx 950 \text{ nm}$  ( $E \approx 1.3 \text{ eV}$ ) is associated with the SP mode of the Ag-quartz interface with  $i^2 + j^2 = 1$ . In the absence of SP interactions, this mode is fourfold degenerate for  $\theta = 0$ . Figures 3 and 4 show that the  $(\pm 1, 0)$  modes have a fairly large dispersion, while for small  $k_x$  the  $(0, \pm 1)$  modes show no dispersion since only the  $x$  component of the wave vector is changed.

We identify the transmission minima as the result of Wood's anomaly,<sup>11</sup> which was observed in diffraction gratings and occurs when a diffracted order becomes tangent to the plane of the grating. When the order disappears, the light intensity is redistributed among the remaining orders; it has been suggested<sup>13</sup> that the intensity in the grazing order shows a significant increase before being extinguished, causing an anomalous reduction in the lower-order intensities. The condition for Wood's anomaly is similar to Eq. (1), but instead of creating a surface plasmon mode with wave vector  $k_{sp}$ , a diffracted wave grazes the surface, in a direction given by  $(i, j)$ . The wave vector of the grazing light is given by  $k_{diff} = n\omega/c = 2\pi n/\lambda$ , where  $n = \sqrt{\epsilon_1}$  is the index of refraction of the dielectric medium (either  $n = 1$  for air or  $n = 1.47$  for quartz), assuming absorption can be ignored. For the one-dimensional case  $i = 0$ , Eq. (3) reduces to the familiar condition  $j\lambda = na_0$ . (In treating the orders that are diffracted into the dielectric, one has to take into account the diffraction at the quartz-air interface, governed by Snell's law; we note that the abscissa of Figs. 3 and 4 is  $k_x = k_0 \sin \theta$ , where  $\theta$  is measured in air.) The dashed markers in Fig. 2 and the dashed lines in Fig. 4 show the loci of Wood's anomaly calculated for a square array with period  $a_0 = 600 \text{ nm}$ .

As an example we consider again the case of  $i^2 + j^2 = 1$  for the quartz-metal interface ( $\lambda = na_0 = 882 \text{ nm}$  or  $E \approx 1.4 \text{ eV}$ ; see Figs. 2–4). This minimum has a fourfold degeneracy for  $\theta = 0$  since the diffracted beams are grazing for  $(i, j) = (\pm 1, 0)$  and  $(0, \pm 1)$ . As the incident angle  $\theta$  becomes finite, the  $(1, 0)$  mode emerges from the surface and a longer wavelength is required to make it grazing again; the opposite holds for the  $(-1, 0)$  mode, which requires a shorter wavelength in order to graze the surface. As in the case of the SP dispersion, at small  $\theta$  the  $(0, \pm 1)$  modes remain at the same  $\lambda$  since the sample is rotated about the  $y$  axis and only the diffraction in the  $x$  direction is affected.

Figure 4 shows the very good agreement between the data and the predicted loci for Wood's anomaly for the minima at  $\lambda \geq 0.5 \mu\text{m}$ . At shorter wavelengths (higher photon energy) both maxima and minima occur so close together that they are not resolved in our measurement. It is surprising to see the equally good agreement to the dispersion of the surface plasmons according to Eqs. (1) and (2), especially since the latter does not take into account the presence of the holes. These are expected to lead both to coupling of surface plasmon modes on the same surface, as well as coupling of modes on both sides of the metal film. The symmetry of the transmission with respect to the illumination side shows that this coupling is extremely strong, which should lead to large level repulsions or energy gaps in the dispersion relation. While we estimated the size of the gaps earlier,<sup>9</sup> it is now clear that the presence of Wood's anomaly prevents the direct measurements of such gaps. The width of the minima is limited by the dispersion  $\delta k$  of the incident beam, consistent with the Wood's anomaly being a purely geometric effect. In contrast, the width of the maxima is not limited by the resolution of this experiment. The peak widths may be due to inhomogeneous broadening from irregularities in the holes or alternatively they may reflect the lifetime of the surface plasmons.<sup>14</sup>

It is useful to compare the hole arrays with several other structures. Transmission efficiencies approaching unity have been reported in a smooth (unmodulated) silver film, but only at small film thickness ( $t=600$  Å) and in a symmetric situation in which the dielectric constant of the adjacent media must be identical.<sup>15</sup> In contrast, in the work reported here, the transmission enhancement is mediated by the strong coupling of surface plasmon modes on both sides of the metal film through the holes, despite the fact that the film thickness far exceeds the skin depth of the metal ( $\sim 20$  nm), and the media on the two sides have significantly different indices of refraction. In addition, in the transmission spectra of a one-dimensional array of gold wires,<sup>16</sup> a resonant absorption (rather than transmission) feature has been identified with a surface plasmon resonance. In that system the gold wires are isolated from one another, unlike the case for our multiply connected film. Another relevant class of structures are periodic multielectric structures, in which coherent backscattering leads to the formation of photonic bands and band gaps, similar to the formation of energy bands for electrons in crystalline solids.<sup>17</sup> Such structures can be manipu-

lated to allow the selective transmission of photons traveling in the plane of the modulation.<sup>17-19</sup> In contrast, even though the surface plasmons in our films are confined to the metal surfaces, their interactions with the incident radiation leads to selectively enhanced transmission in a direction normal to the plane of the film.

The very high transmission efficiencies, together with the subwavelength resolution, make these structures attractive for possible application in nanofabrication technology. A detailed understanding of the mechanism leading to the enhanced transmission will require a rigorous theory, which must take into account the anomalous coupling of the SP modes on both metal surfaces through the holes. Experiments are now under way which are expected to elucidate the coupling between the surface plasmon modes on the two surfaces of the metal film.

We thank P. A. Wolff, J. A. Giordmaine, M. M. J. Treacy, R. A. Linke, and D. J. Chadi for discussions. We are particularly grateful to P. A. Wolff for suggesting surface plasmons as a mechanism for enhanced transmission.

<sup>1</sup>H. Raether, *Surface Plasmons* (Springer-Verlag, Berlin, 1988).

<sup>2</sup>R. H. Ritchie, E. T. Arakawa, J. J. Cowan, and R. N. Hamm, *Phys. Rev. Lett.* **21**, 1530 (1961).

<sup>3</sup>M. C. Hutley and V. M. Bird, *Opt. Acta* **20**, 771 (1973).

<sup>4</sup>T. Inagaki, J. P. Goudonnet, J. W. Little, and E. T. Arakawa, *J. Opt. Soc. Am. A* **2**, 433 (1985).

<sup>5</sup>Y. J. Chen, E. S. Koteles, R. J. Seymour, G. J. Sonek, and J. M. Ballantine, *Solid State Commun.* **46**, 95 (1983).

<sup>6</sup>R. A. Watts, J. B. Harris, A. P. Hibbins, T. W. Preist, and J. R. Sambles, *J. Mod. Opt.* **43**, 1351 (1996).

<sup>7</sup>G. H. Derrick, R. C. McPhedran, D. Maystre, and M. Neviere, *Appl. Phys.* **18**, 39 (1979).

<sup>8</sup>A. Hessel and A. A. Oliner, *Appl. Opt.* **4**, 1275 (1965).

<sup>9</sup>T. W. Ebbesen, H. J. Lezec, H. F. Ghaemi, T. Thio, and P. A. Wolff, *Nature (London)* **391**, 667 (1998).

<sup>10</sup>H. A. Bethe, *Phys. Rev.* **66**, 163 (1944).

<sup>11</sup>R. W. Wood, *Philos. Mag.* **4**, 396 (1902); R. W. Wood, *Phys. Rev.* **48**, 928 (1935).

<sup>12</sup>D. W. Lynch and W. R. Hunter, in *Handbook of Optical Constants of Solids*, edited by E. D. Palik (Academic, Orlando, 1985).

<sup>13</sup>Lord Rayleigh, *Proc. R. Soc. London, Ser. A* **79**, 399 (1907).

<sup>14</sup>M. van Exter and A. Lagendijk, *Phys. Rev. Lett.* **60**, 49 (1988).

<sup>15</sup>R. Dragila, B. Luther-Davies, and S. Vukovic, *Phys. Rev. Lett.* **55**, 1117 (1985).

<sup>16</sup>H. Lochbihler, *Phys. Rev. B* **50**, 4795 (1994).

<sup>17</sup>J. D. Joannopoulos, P. R. Villeneuve, and S. Fan, *Nature (London)* **386**, 143 (1997).

<sup>18</sup>S. C. Kitson, W. L. Barnes, and J. R. Sambles, *Phys. Rev. Lett.* **77**, 2670 (1996).

<sup>19</sup>J. S. Foresi, R. P. Villeneuve, J. Ferrera, E. R. Thoen, G. Steinmeyer, S. Fan, J. D. Joannopoulos, L. C. Kimerling, H. I. Smith, and E. P. Ippen, *Nature (London)* **390**, 143 (1997).